Influence of Processing Conditions on Melt Blown Web Structure: Part 2 – Primary Airflow Rate

By Randall R. Bresee, Department of Materials Science & Engineering, The University of Tennessee, Knoxville, Tennessee and Uzair A. Qureshi and Matthew C. Pelham, Jentex Corporation, Buford, Georgia

Abstract

We are continuing an effort to quantitatively measure the influence of processing variables on the detailed structure of commercial polypropylene melt blown (MB) webs. In this paper, we report the influence of primary airflow rate on fiber entanglement, global fiber orientation and pore structure in webs. This enabled us to quantify the influence of primary airflow on web structural features as well as achieve greater understanding of the commercial MB process.

Key Words

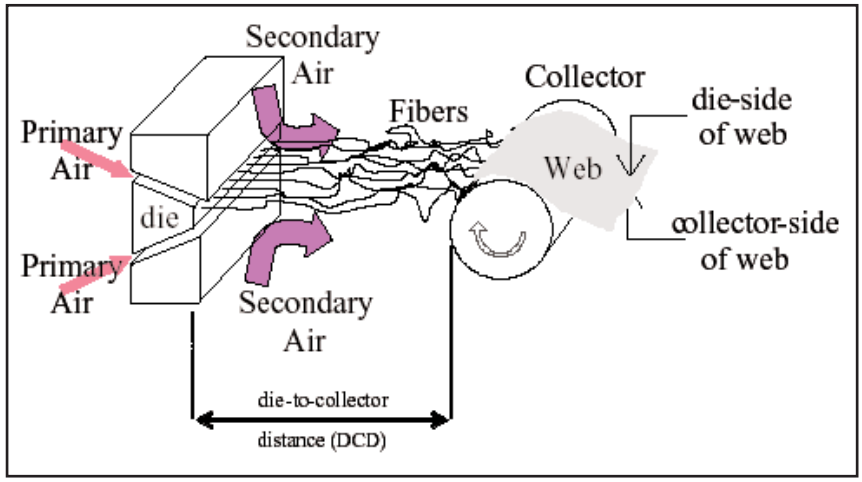
melt blowing, web, processing, primary airflow, fiber entanglement, fiber orientation, pore, bundle.

Introduction

Melt blowing (MB) combines fiber extrusion, fiber diameter attenuation, development of molecular orientation, polymer crystallization and fabric formation into a one-step process. The concurrent nature and fast speed of these complex events makes MB difficult to understand. When melted polymer is pumped through die orifices, it enters high-speed streams of hot air, called primary air, as illustrated in *Figure 1*. When melted filaments initially emerge from the die, their speed is slow and the speed of primary air is very fast so airflow drags the fibers in the general direction of airflow, which is the machine direction (MD). At increasing distance from the die, air speed decreases and fiber speed increases so the maximum fiber speed is achieved at about 6 cm from the die [1]. At distances greater than this, mean air speed and mean fiber speed are similar and both decrease at all subsequent locations en route to the collector. It is important to recognize that fiber speed increases through relatively little of the die-collector space and decreases through most of the space between the die and collector. It also is important to recognize that the temperature of fibers moving away from the die decreases as they encounter increasing amounts of cooler secondary air. Secondary air usually is drawn from the ambient environment near the MB equipment but may sometimes be chilled.

These general considerations lead us to expect that, near the die, primary airflow will dominate many other processing

Figure 1
ILLUSTRATION OF THE BASIC MELT BLOWING PROCESS



FITESA/Exhibit 1026, Page 1 of 8

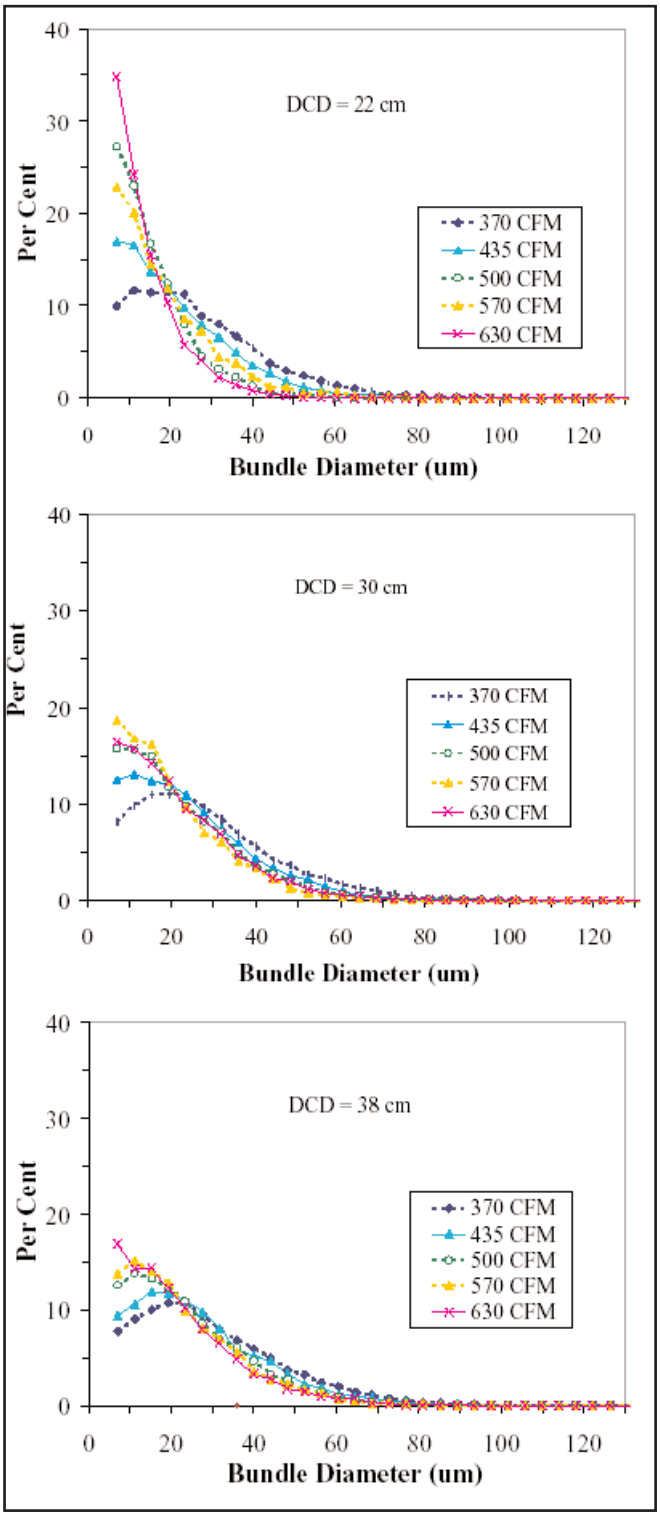


Figure 2
FIBER BUNDLE SIZE DISTRIBUTIONS AT VARIOUS PRIMARY AIRFLOW RATES (FT^3/MIN) FOR 22 CM, 30 CM AND 38 CM DCD

variables affecting fiber and web properties since most of the air interacting with fibers is primary air and air speed exceeds fiber speed significantly. We also should expect primary airflow to play a substantially less dominant role at locations not near the die since much secondary air is mixed with primary air and air speed is similar to fiber speed.

Fabric formation (i.e. a fiber network) begins to develop within 1 cm of the die but network structure is dynamic and becomes fixed only when fibers contact the collector and their motion ceases. Consequently, numerous polymer, air and equipment variables influence web structure development and changes in nearly any variable may influence web structure in a complicated way. This leads us to expect that the MB process will surrender its secrets only grudgingly.

We recently began an effort to quantitatively determine the influence of major processing variables on the structure of webs produced by the commercial MB process. In a previous paper, we reported the influence of die-to-collector distance (DCD) on fiber entanglement, global fiber orientation and pore structure in webs [2]. In this paper, we address the influence of primary airflow rate on these same web structural features. Although a wide variety of materials have been MB (e.g. carbon pitch, elastomers, polyesters, polyamides and others), polypropylene is the most commonly used polymer for MB because of its low cost and the availability of resin grades developed specifically for MB. Consequently, we have used polypropylene in our study. We hope this work leads us to detailed and quantitative knowledge of the influence of processing variables on web structure as well as greater understanding of the commercial MB process.

Experimental Procedures

We prepared thirty 21 g/m^2 webs using ExxonMobil 3505GE1 polypropylene of 400 melt flow rate. The MB line used to prepare webs was a 115 cm (45 inch) wide horizontal commercial MB line with a 200 cm (79 inch) diameter rotating drum collector. The die had 14 holes/cm (35 holes/inch) with hole diameters of 305 μm (0.0120 inch). We varied primary airflow rate from 370 to 700 ft^3/min by varying primary air pressure. Die-to-collector-distances were varied from 22 to 40 cm (8.5-15.0 inch). Resin throughput rate remained constant.

Fiber bundle analysis [3], fiber orientation analysis [3] and pore analysis [4] were measured off-line quantitatively from fully-formed webs using WebPro, an automated image analysis-based instrument [5]. A substantial effort was made to sample web structure adequately. This involved evaluating approximately 600 locations for fiber entanglement analysis, 600 locations for fiber orientation analysis and 400 locations for pore analysis in each web.

Results and Discussion

The discussion below addresses the influence of primary airflow rate on the structure of fully-formed webs produced by a commercial MB process. We will discuss how airflow rate influences fiber entanglement, fiber orientation and pore structure in webs.

Fiber Entanglement

Fibers commonly become entangled during processing into cohesive, tight fiber groups called bundles. From an analytical point of view, bundles may be composed of a single fiber

FITESA/Exhibit 1026, Page 2 of 8

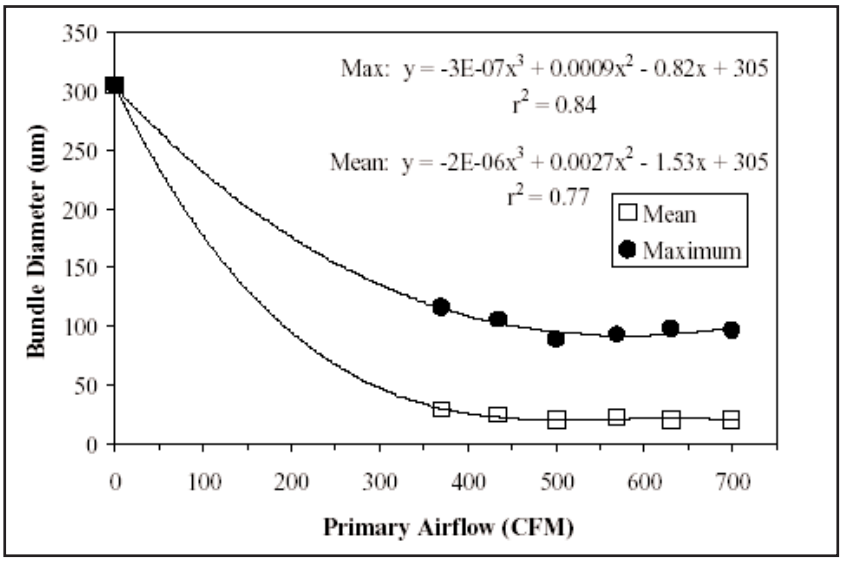


Figure 3
CURVES FITTED TO MAXIMUM AND MEAN FIBER BUNDLE SIZE AVERAGED FOR FIVE DCD'S AT EACH PRIMARY AIRFLOW RATE

(entanglement of one) or a very large number of fibers. When fiber entanglement increases, the number and size of fiber bundles increase. We assessed fiber entanglement by evaluating the size of fiber bundles at 600 locations across the full width of each web. *Figure 2* shows fiber bundle diameter distributions for various primary airflow rates and a relatively short DCD (22 cm), medium DCD (30 cm) and long DCD (38 cm).

Mean and maximum bundle diameters were determined for each distribution and then averaged for the five DCD's we used at each primary airflow rate to reduce data noise. We searched for equations that fit the data after fixing the y-intercept at 305 μm. This fixed mean and maximum bundle diameters equal to the die orifice diameter when primary airflow was zero and no fiber drawing or entanglement was expected. *Figure 3* provides these results along with third order polynomial fits to our data (r^2 = 0.84 and 0.77). This figure provides reasonable functional forms for evaluating the influence of primary airflow on fiber bundle size.

Figure 2 clearly shows that fiber entanglement depended on primary airflow rate at all DCD's and *Figures 2-3* indicate that fiber entanglement was reduced when primary airflow rate was increased. In particular, Figure 2 shows that the percentage of coarse fiber bundles decreased and the percentage of fine fiber bundles increased when primary airflow rate was increased. Several factors may contribute to these experimental observations.

First, any process change that produces finer individual filaments will increase the number of fine bundles and reduce the number of coarse bundles. It is well known that increasing primary airflow rate reduces fiber diameter and thus reduces fiber bundle size.

Second, it takes time for fiber entanglement to occur so any process change that decreases fiber travel time reduces the number of coarse bundles and increases the relative number of fine bundles. It is well known that increasing primary airflow rate increases fiber velocity in the MD and thus reduces fiber travel time to the collector. In addition, increasing primary airflow in the MD should have a similar affect on fiber entanglement as reducing DCD since both of these reduce fiber travel time.

Third, increasing airflow at the die increases airflow at the collector. Since airflow diverges substantially over the collector surface [6] and fiber flow tends to follow airflow, increasing primary airflow at the die increases fiber flow divergence near the collector. This reduces fiber entanglement near the collector since fiber flow is dispersed through a larger region of space.

Figure 2 also shows that primary airflow had a more substantial influence on fiber entanglement when DCD was smaller. For example, varying airflow between 370 ft^3/min and 630 ft^3/min caused the percentage of bundles in the 9-13 μm size interval to vary 12.6 % (11.7% to 24.3%) for webs produced with 22 cm DCD, 6.0% (9.8% to 15.8%) for webs produced with 30 cm DCD and 5.2% (9.1% to 14.3%) for webs produced with 38 DCD. Since fiber entanglement affects nearly every web structural feature or web property, the uniformity of primary airflow is particularly important for webs produced with shorter DCD's. Fiber entanglement occurs for many reasons and is influenced by numerous process variables [1,7,8]. However, we should generally expect primary airflow to be a particularly important influence on fiber entanglement at shorter DCD's.

Figure 2 also shows that primary airflow influenced smaller bundle sizes substantially more than larger bundle sizes. For example, varying primary airflow between 370 ft^3/min and 630 ft^3/min for the 22 cm DCD webs caused the percentage of bundles in the 5-9 μm size interval to vary substantially (9.9% to 34.8%) whereas the percentage of bundles in the 30-34 μm size interval varied moderately (8.0% to 2.2%). To understand this, we should note that fiber bundles range from single fibers (an entanglement of one) to large entanglements composed of many fibers. Increasing primary airflow reduces single fiber diameter and the majority of this diameter attenuation occurs close to the die before a substantial amount of fiber entanglement occurs. On the other hand, the size of larger fiber bundles is determined by fiber entanglement that occurs mostly far from the die so we should expect the size of larger fiber bundles to depend less on primary airflow. Consequently, primary airflow changes influence the diameters of small fiber bundles (one or a few fibers) more than the diameters of large fiber bundles.

Overall, it is clear that primary airflow affected fiber entanglement significantly. Since entanglement affects nearly every web structural feature and web property, comprehending this phenomenon is important for understanding the MB process.

FITESA/Exhibit 1026, Page 3 of 8

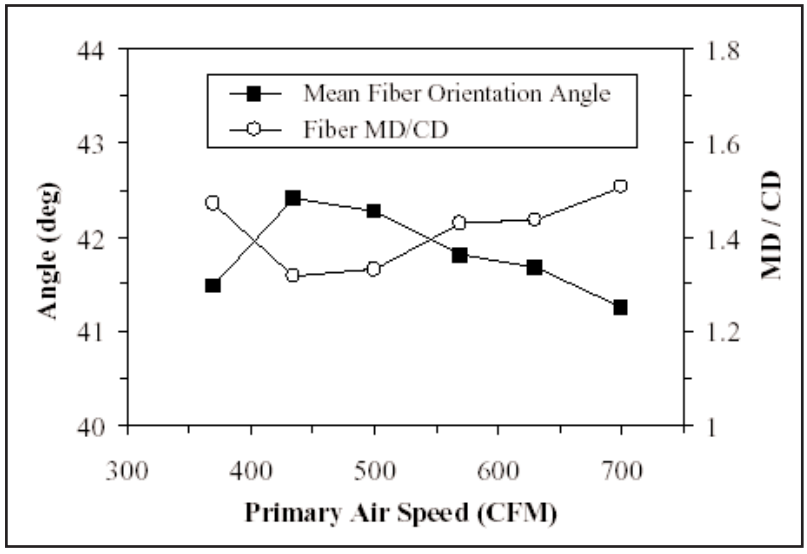


Figure 4
MEAN FIBER ORIENTATION ANGLE AND FIBER MD/CD ORIENTATION RATIO AVERAGED FOR FIVE DCD'S AT EACH PRIMARY AIRFLOW RATE.

For example, it seems likely that increasing primary airflow improves web basis weight uniformity because fiber entanglement is reduced as well as because finer fibers are produced.

Global Fiber Orientation

Melt blown webs typically exhibit broad fiber diameter distributions. Consequently, it is generally more meaningful to assess global fiber orientation in terms of the amount of fiber diameter aligned in various directions rather than the number of fibers aligned in various directions. We simultaneously measured the orientation direction and diameter of numerous fibers at 600 locations across the full width of each web. For these measurements, 0° was defined as the machine direction (MD) and +/- 90° was defined as the cross-machine direction (CD). Once measurements were obtained for several thousand fibers for each web, we computed two simple measures of fiber orientation.

The mean orientation angle was computed from fiber diameter-based orientation data using absolute values of orientation angles. When this was done, the mean fiber orientation angle represented the average orientation angle of all fiber diameter and equaled 45° for isotropic fiber orientation, was less than 45° for preferred MD orientation and was greater than 45° for preferred CD orientation. The MD/CD ratio also was computed from fiber orientation measurements. This represented the amount of fiber diameter oriented near the machine direction (MD +/-20°) divided by the amount of fiber cross-sectional area oriented near the cross direction (CD +/-20°). When this was done, the MD/CD ratio equaled one for isotropic fiber orientation, exceeded one for preferred MD orientation and was less than one for preferred CD orientation. These two measures of fiber orientation represent different things physically but provide similar results for most but not all webs. That is, the mean angle is based on the orientation of all measured fibers whereas the MD/CD ratio is based on only some fibers.

To reduce data noise, we averaged mean orientation angles and MD/CD values for webs produced with the five DCD's we used at each primary airflow rate. These results are provided in *Figure* 4. As is usual for MB webs, all of our webs exhibited preferential MD fiber orientation since mean orientation angles were less than 45° and MD/CD ratios exceeded one in all cases. *Figure 4* shows that global fiber orientation generally increased as primary airflow was increased.

Since web structure is dynamic and becomes fixed only when fibers contact the collector, the state of fiber orientation in fully-formed webs is dominated by fiber motion near the collector rather than fiber motion near the die. However, increasing primary air speed at the die increases the speed of air arriving at the collector. Since fiber speed decreases to zero during laydown, faster air speed at the collector increases drag force during laydown. Consequently, increasing primary airflow rate increases the tendency of fibers to be dragged in the general direction of airflow during laydown. Since the direction of airflow in the laydown region of a rotating drum collector of the basic MB process is the MD, increasing primary airflow ought to increase MD orientation in webs. Figure 4 shows that global fiber orientation generally increased as primary airflow was increased.

Figure 4 also shows that the low end of our airflow region (370 ft^3/min) did not exhibit the pattern observed at higher airflow rates. To examine the possibility that an errant measurement produced this inconsistency, we provide MD/CD orientation data points for individual webs in *Figure 5*. When primary airflow was increased from 370 to 435 ft^3/min, this figure shows that fiber orientation decreased for all five web series. When mean fiber orientation angle data were viewed similarly, fiber orientation decreased for four of the five web series when airflow was increased from 370 to 435 ft^3/min. These observations indicate that the fiber orientation reduction observed when primary airflow rate was increased from 370 to 435 ft^3/min is likely correct. Unfortunately, we are unable to identify the cause of this phenomenon without additional observations.

Figure 5 is useful for obtaining insight into another phenomenon. This figure shows that data points within individual DCD series seemed to vary over a larger range when webs were collected at smaller DCD's. Mean fiber orientation angle data also exhibited larger variations when webs were collected at smaller DCD's. These observations suggest that less stable conditions may have existed during fiber laydown when DCD was smaller. Thus, careful measurements of web struc-

FITESA/Exhibit 1026, Page 4 of 8

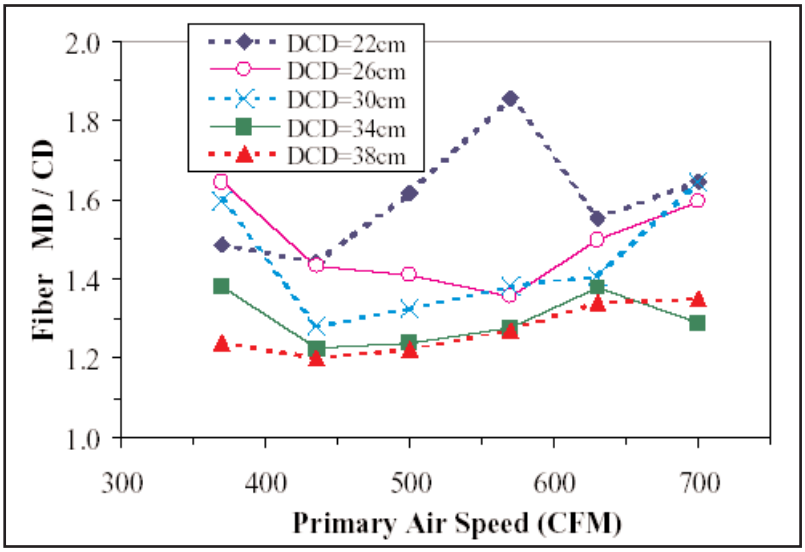


Figure 5
MD/CD ORIENTATION RATIO AT EACH PRIMARY AIRFLOW RATE AND DCD

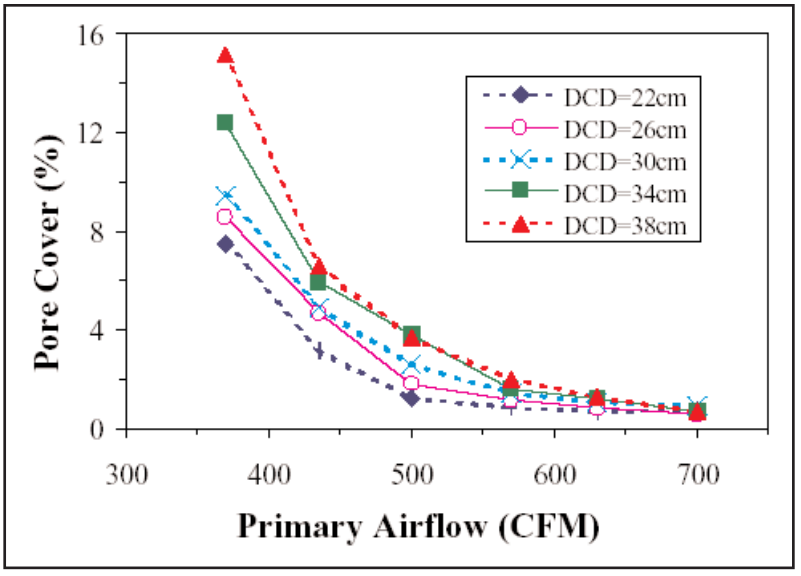


Figure 6
PORE COVER AT EACH PRIMARY AIRFLOW RATE AND DCD

ture may provide evidence of fiber flow instability during laydown.

Overall, the influence of primary airflow rate on web structure seems to be complicated. We were able to explain the general trend in fiber orientation as a function of primary airflow but were unable to explain the deviation from this trend at the lowest airflow rate we used. Our study also provided evidence that fiber flow instability may have existed during laydown at small DCD's and could possibly be monitored by careful fiber orientation measurements. It is apparent that more detailed studies of primary airflow rate are required to achieve a better understanding of its influence on global fiber orientation.

Pore Structure

The size and shape of numerous individual pores were measured at 400 locations across the full width of each web. Pore measurements obtained in this manner were physically meaningful only for relatively thin webs where pores are approximately two-dimensional. Webs produced for our study were relatively thin (basis weights were 21 g/m^2) so physical interpretation of pore measurements was relatively straightforward.

Once pore measurements were obtained for many thousands of individual pores for each web, pore cover was computed. Pore cover represents the percentage of web area that is covered with pores rather than fibers (pore cover + fiber cover = 100%). *Figure 6* provides pore cover data for various primary airflow rates and DCD's. This figure shows that primary airflow influenced pore cover substantially. Changes in primary airflow rate influenced pore cover most when airflow was smaller and when DCD was larger. *Figure 6* also shows that DCD influenced pore cover most when primary airflow rate was smaller and when DCD was larger. The influence of both primary airflow and DCD on pore cover became diminished at larger airflow rates and smaller DCD's. These observations are reasonable since the structure of webs is determined largely by drag forces acting on fibers during laydown. These forces are determined mostly by air speed near the collector which, in turn, is determined by primary airflow.

Figure 6 also indicates that primary airflow rate and DCD could influence pore cover roughly similar amounts, depending on the processing conditions used. For example, when DCD was large (38 cm) and primary airflow rate was increased 18% (from 370 ft^3/min to 435 ft^3/min), pore cover was reduced by 57% (from 15.2% to 6.6%). In comparison, when primary airflow rate was small (370 ft3/min) and DCD was decreased 21% (from 38 cm to 30 cm), pore cover was reduced by 38% (from 15.2% to 9.4%).

The five DCD data points in *Figure 6* at each airflow rate were averaged and then a polynomial was fitted to the averages after fixing the y-intercept at a pore cover value of 58%. This value corresponded to the pore cover computed after assuming that fiber diameter equaled the die orifice diameter (305 μm) when primary airflow was zero and no fiber entanglement occurred. A good fit (r^2 = 0.98) to the data was obtained with a third order polynomial as the dashed line in *Figure 7* shows.

Fiber entanglement data from *Figure 3* (mean bundle diameters) were replotted in *Figure 7* to facilitate comparison with pore cover. The general similarities of the two curves in *Figure 7* suggest that pore cover was strongly influenced by fiber

FITESA/Exhibit 1026, Page 5 of 8

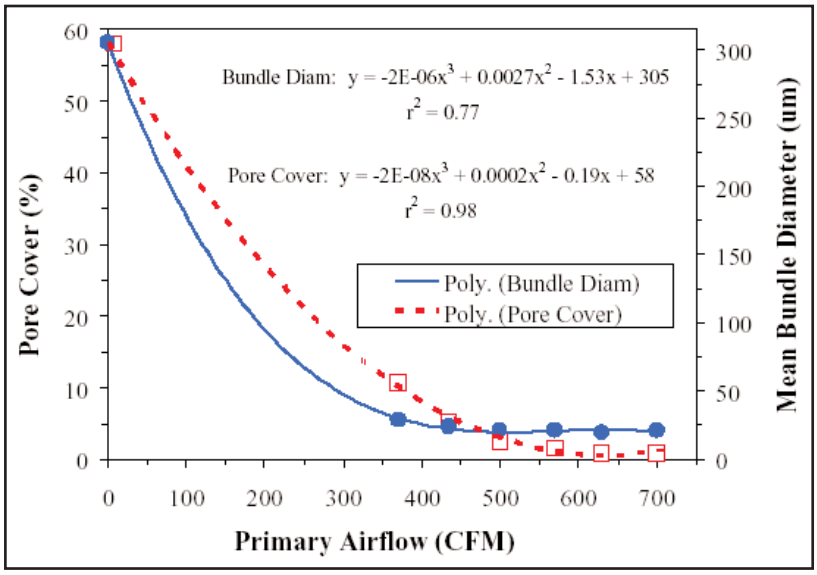


Figure 7
CURVES FITTED TO PORE COVER (DASHED LINE) AND MEAN FIBER BUNDLE SIZE (SOLID LINE) AVERAGED FOR FIVE DCD'S AT EACH PRIMARY AIRFLOW RATE

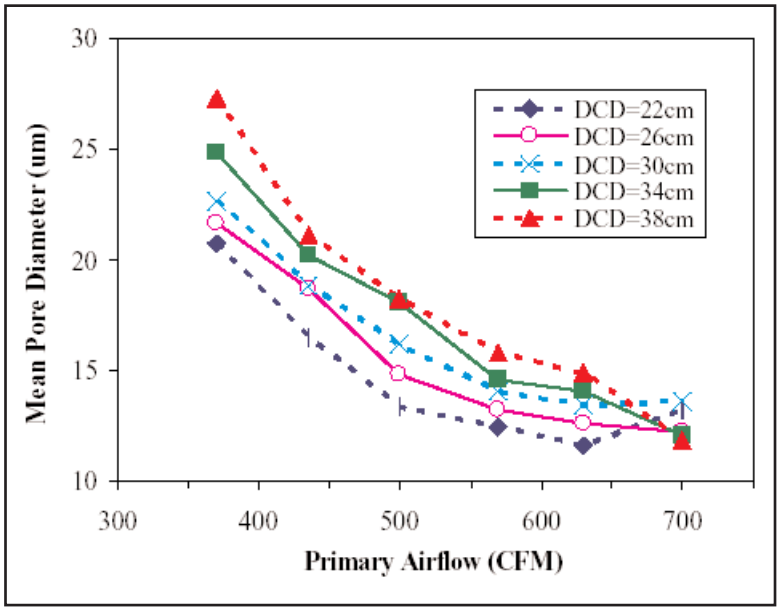


Figure 8
MEAN PORE SIZE AT EACH PRIMARY AIRFLOW RATE AND DCD

entanglement. Higher primary airflow rates reduced fiber entanglement which, in turn, increased effective fiber cover and thus reduced pore cover. However, *Figure 7* also indicates that other web structural features must contribute to pore cover since the two curves differ. For example, pore cover continued to decrease when primary airflow was increased whereas fiber bundle size leveled off at a moderate airflow rate (500 ft^3/min). It is likely that single fiber diameter differences contributed to the continued reduction in pore cover when primary airflow was increased. It is well known that greater primary airflow rates produce finer fiber diameters which, in turn, increase fiber cover and reduce pore cover. We will conduct fiber diameter analysis in the future in an attempt to quantitatively evaluate its contribution to pore cover.

Pore cover data can be interpreted further by examining the two basic structural features that contribute most to pore cover - pore size and the number of pores. Pore size data are provided in *Figure 8* in terms of the mean pore diameter (equivalent circle diameter) for each web. This figure shows that pore size was influenced markedly by primary airflow.

Comparison of *Figures 6 and 8* shows that general trends for pore cover and pore size were quite similar. That is, both pore cover and pore size were generally larger for webs produced with larger DCD's and decreased when primary airflow rate was increased at any particular DCD. These similarities suggest that the affects of primary airflow and DCD on pore cover were related to their influence on pore size.

Figure 9 provides the number of pores per unit web area for each web. Like mean pore size, this figure shows that the number of pores detected by optical microscopy was markedly influenced by primary airflow rate. This is reasonable since increasing primary airflow rate produces finer fiber diameters and thus increases the amount of fiber length per unit web area. In webs containing moderate-sized pores, the production of finer fibers would be expected to decrease the size of pores and thus reduce the number of pores detected by optical microscopy.

Comparison of *Figures 6 and 9* shows that trends for pore cover and the number of pores were similar when primary airflow rate is considered and DCD is ignored. This suggests that the affect of primary airflow on pore cover was related to its influence on the number of pores. In contrast to this, comparison of *Figures 6 and 9* shows that trends were substantially different when DCD is considered. That is, pore cover was consistently larger for webs produced with larger DCD's *(Figure 6)* whereas the number of pores was not consistently larger for webs produced with larger DCD's *(Figure 9)*. This leads us to conclude that the number of pores in webs is influenced more strongly by primary airflow rate than by DCD. This is reasonable since one would expect the number of pores to depend primarily on the amount of fiber length in a unit web area and fiber diameter has been shown to change only slightly with DCD for distances well beyond the die [7].

Next, we examined the influence of primary airflow rate on the shape of pores. *Figure 10* provides the mean pore aspect ratio averaged for five DCD's at each primary airflow rate. Since circularly-shaped objects exhibit aspect ratios of one,

FITESA/Exhibit 1026, Page 6 of 8

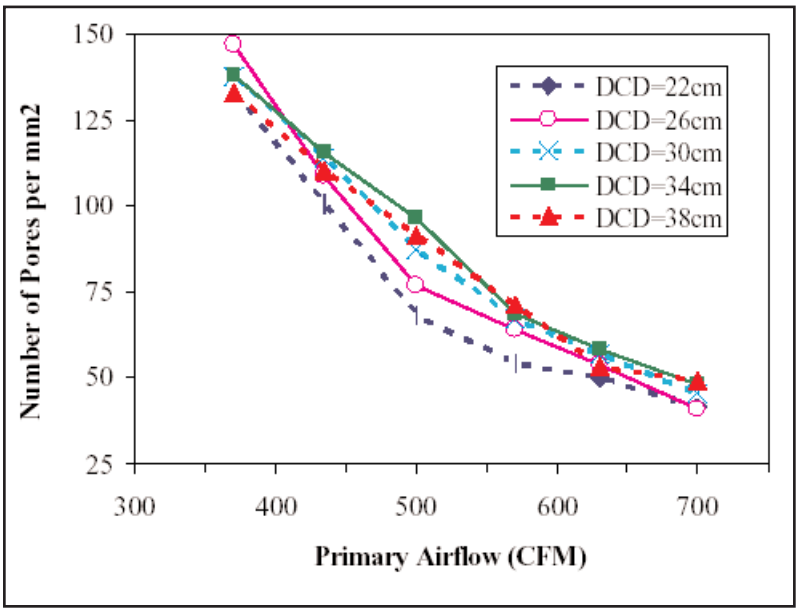


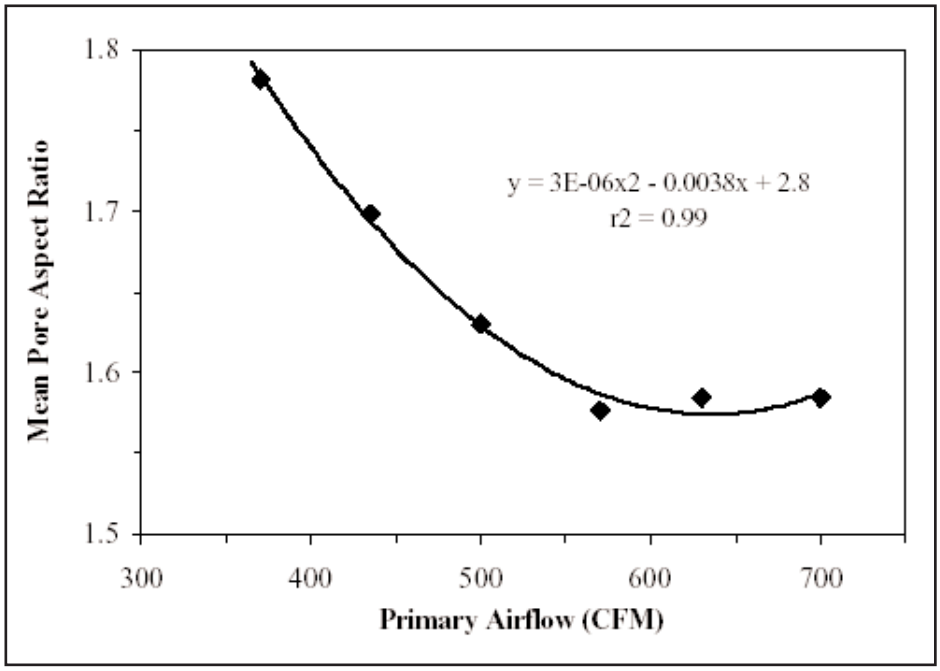
Figure 9
NUMBER OF PORES PER MM² WEB AREA AT EACH PRIMARY AIRFLOW RATE AND DCD

this figure shows that, on average, pores in our MB webs were substantially elongated.

A previous study of the influence of DCD on web structure reported that pore shape did not correlate well with global fiber orientation but instead correlated with local fiber orientation through the variable, fiber bundle size [2]. Fiber entanglement produces fibers that are arranged predominantly in a collinear manner in individual bundles. Nearly parallel arrangements of fibers produce pores that are substantially elongated and causes pore shape to be correlated with local rather than global fiber orientation. In the current study, we again find that pore shape did not correlate well with global fiber orientation and we find again that pore shape did correlate with fiber bundle size. *Figure 10* shows that increasing primary airflow rate reduced pore aspect ratio and *Figure 3* showed that increasing primary airflow rate reduced fiber entanglement. In contrast, *Figure 4* showed that increasing primary airflow generally increased global fiber orientation.

Overall, our data indicate that increasing primary airflow reduced pore cover by decreasing fiber entanglement as well as reducing fiber diameter. The affect of airflow on pore cover was likely related to its influence on both the size and the number of pores. Pore aspect ratio correlated with fiber bundle size rather than global fiber orientation.

Figure 10
MEAN PORE SHAPE AVERAGED FOR FIVE DCD'S AT EACH PRIMARY AIRFLOW RATE.



Conclusions

We reported quantitative experimental measurements of the influence of primary airflow rate on fiber entanglement, global fiber orientation and pore structure in webs. Overall, primary airflow effects were complicated. We observed the following specific effects:

Primary airflow affected fiber entanglement significantly. Increasing primary airflow rate reduced fiber entanglement, especially when DCD was shorter. Fine fiber bundles were affected more than coarse bundles when primary airflow was changed. The influence of primary airflow rate on fiber entanglement was reduced at larger airflow rates. Several explanations were thought to be responsible for these experimental observations. Since fiber entanglement affects nearly every web structural feature and web property, this finding is important.

Increasing primary airflow rate generally increased global orientation of fibers in the MD. This was explained on the basis of aerodynamic drag since increasing airflow rate at the die increases the speed of air arriving at the collector so the drag force available to orient fibers in the direction of airflow (MD) during laydown is increased. It was thought that careful measurements of fiber orientation may provide evidence of fiber flow instability during laydown.

Increasing primary airflow rate

FITESA/Exhibit 1026, Page 7 of 8

reduced pore cover in webs substantially. This was thought to occur because increased airflow decreased fiber entanglement and reduced fiber diameter. Airflow influenced pore cover most when primary airflow rate was smaller and when DCD was larger. DCD also influenced pore cover most when primary airflow rate was smaller and when DCD was larger. The influence of both primary airflow and DCD on pore cover became diminished at larger airflow rates and smaller DCD's. Depending on the processing conditions used, primary airflow rate and DCD could influence pore cover roughly similar amounts. Increasing primary airflow rate reduced the size and the number of pores in webs substantially. Increasing primary airflow rate also reduced the aspect ratio of pores. Pore shape correlated with fiber entanglement (bundle size) and did not correlate with global fiber orientation.

References

1. Yin, H., Yan, Z., Ko. W.C. and Bresee, R.R. "Fundamental Description of the Melt Blowing Process," *International Nonwovens Journal*, 9(4) (2000) 25-28

2. Bresee, R.R. and Qureshi, U.A., "Influence of Processing Conditions on Melt Blown Web Structure: Part 1 – DCD," *International Nonwovens Journal*, 13(1) (2004) 49-55

3. Huang, X.C. and Bresee, R.R. "Characterizing Nonwoven Web Structure Using Image Analysis Techniques. Part II: Fiber Orientation Analysis in Thin Webs," *Journal of Nonwovens Research*, 5(2), 14-21 (1993)

4. Huang, X.C. and Bresee, R.R. "Characterizing Nonwoven Web Structure Using Image Analysis Techniques. Part I: Pore Analysis in Thin Webs," *Journal of Nonwovens Research*, 5(1), 13-21 (1993)

5. Yan, Z. and Bresee, R.R. "Flexible Multifunction Instrument for Automated Nonwoven Web Structure Analysis," *Textile Research Journal*, 69, 795-804 (1999)

6. Bresee, R.R. and Qureshi, U.A. "Fiber Motion Near the Collector During Melt Blowing. Part I: General Considerations," *International Nonwovens Journal*, 11(2), 27-34 (2002)

7. Yin, H., Yan, Z. and Bresee, R.R. "Experimental Study of the Melt Blowing Process," *International Nonwovens Journal*, 8(1), 60-65 (1999)

8. Bresee, R.R. and Ko, W.C. "Fiber Formation During Melt Blowing," *International Nonwovens Journal*, 12(2) (2003) 21-28—***INJ***

Return to Table of Contents

FITESA/Exhibit 1026, Page 8 of 8